

Measuring orbital interaction using quantum information theory

Jörg Rissler^{a,*}, Reinhard M. Noack^a, Steven R. White^b

^a*Fachbereich Physik, Philipps-Universität Marburg, D-35032 Marburg, Germany*

^b*Department of Physics and Astronomy, University of California, Irvine CA 92697-4575, USA*

Abstract

Quantum information theory gives rise to a straightforward definition of the interaction of electrons $I_{p,q}$ in two orbitals p, q for a given many-body wave function. A convenient way to calculate the von Neumann entropies needed is presented in this work, and the orbital interaction $I_{p,q}$ is successfully tested for different types of chemical bonds. As an example of an application of $I_{p,q}$ beyond the interpretation of wave functions, $I_{p,q}$ is then used to investigate the ordering problem in the density-matrix renormalization group.

Key words: Quantum-information theory, density-matrix renormalization group, orbital interaction

1 Introduction

Orbital interaction is used mainly as a *qualitative* concept in chemistry. Examples are frontier orbital theory or the isolobal principle. Two orbitals are said to interact when they have similar energy and/or matching spatial distribution and/or matching occupation. This concept is also important in theoretical chemistry: for example, in complete-active-space calculations, one chooses (interacting) orbitals to form the active space. However, there is no unique quantitative measure of orbital interaction.

One way to obtain a quantitative measure of orbital interaction is to utilise the concept of entanglement. Namely, if one divides the Hilbert space for a

* Fax:++49-6421-28-24511

Email address: rissler@staff.uni-marburg.de (Jörg Rissler).

given correlated wave function into two parts, then one can determine the entanglement of the two parts for the given wave function. For example, a division of a Hilbert space into one orbital and the space spanned by all the other orbitals defines the entanglement of this specific orbital with the rest of the Hilbert space. The more an orbital is entangled, the more it exchanges information with the other orbitals within the wave function. It is therefore natural to identify entanglement with orbital interaction. The advantage of this interpretation is that quantum information theory [1,2] defines a *quantitative* measure of the entanglement and hence of orbital interaction: the von Neumann entropy S . The disadvantage of using such a definition in calculations is that S is a function of density-matrix eigenvalues. Consequently, a correlated wave function must be obtained before a von Neumann entropy can be calculated.

In order to proceed, one must use a method that produces an approximate wave function from which the von Neumann entropies can be calculated in a simple fashion. In addition, the approximate results should be close to those for the exact wave function. One suitable technique is to solve the full-configuration-interaction (FCI) problem using the density-matrix renormalization group (DMRG) [3]. This method produces wave functions and energies with a well-defined error. In addition to control of the accuracy of the wave function, the DMRG allows easy access to operators and expectation values in second-quantised form. We use this approach in order to calculate the von Neumann entropies in a straightforward way.

In the following, we argue that a reliable measure of the orbital interaction between two orbitals can be formed by subtracting the von Neumann entropy of the two orbitals taken together from the sum of the individual von Neumann entropies of each orbital. We then explore the utility of this measure and how their properties depend on the accuracy of the wave function, we investigate four example molecules which contain different types of chemical bonds: LiF, CO, N₂, and F₂. It turns out that the results do not depend significantly on the accuracy of the wave function. It is therefore sufficient to determine the orbital interaction using a comparatively inexpensive calculation.

We then apply this definition of orbital interaction to a problem in theoretical chemistry: namely, the ordering problem in the DMRG algorithm. One ingredient needed to define the DMRG algorithm is to order the orbitals that span the Hilbert space onto a one-dimensional lattice. This ordering has a significant influence on the convergence of the energy. In order to find an ordering that ensures a good convergence, the literature offers several approaches [4,5], which all have one aspect in common: they define a measure of orbital interaction and order the orbitals in a way so that strongly interacting orbitals are near each other. Therefore, the measure of orbital interaction defined in this work opens up a new way of approaching this problem.

These topics are treated in the following order: First, an introduction to the calculation of von Neumann entropies and a definition of the orbital interaction is given in Section 2, which also contains a recipe for calculating these quantities using expectation values of operators in second quantisation. Section 3 presents the aspects of the DMRG relevant for this work. Subsequently, the orbital interaction is calculated for a set of test molecules in Section 4 in order to test the reliability of the proposed method. Section 5 then presents results for the ordering problem in the DMRG. Finally, the main findings are summarised in Section 6.

2 Entanglement and orbital interaction

2.1 Definition of the orbital interaction $I_{p,q}$

It is useful to divide the Hilbert space of a quantum-mechanical problem (the “universe”) into two parts, which we will call the “system” and the “environment”. If the basis of the system is described by a complete set of states $\{|i\rangle\}$ and that of the environment is described by the set $\{|j\rangle\}$, the general wave function $|\Psi\rangle$ can be written as [6]

$$|\Psi\rangle = \sum_{i,j} C_{i,j} |i\rangle |j\rangle . \quad (1)$$

With the help of the density operator for a pure state describing the total problem $\hat{\rho} = |\Psi\rangle\langle\Psi|$, one can express the reduced density matrix for the system as

$$\rho_{i,i'}^{\text{sys}} = \sum_j \rho_{ij,i'j} = \sum_j \langle j| \langle i| \Psi\rangle\langle\Psi|i'\rangle |j\rangle = \sum_{j,i'} C_{i,j}^* C_{i',j} . \quad (2)$$

This is the typical way to set up reduced density matrices. It requires the partition of the wave function as in Eq. (1) as well as the knowledge of the coefficients $C_{i,j}$.

It is also possible, however, to formulate the problem in a different way. Suppose one has another, arbitrary basis for the system, $\{|n\rangle\}$, then

$$\rho_{n,n'}^{\text{sys}} = \sum_j \rho_{nj,n'j} = \sum_j \langle j| \langle n| \Psi\rangle\langle\Psi|n'\rangle |j\rangle . \quad (3)$$

With the help of Eq. (1) one can write

$$\rho_{n,n'}^{\text{sys}} = \sum_{j,i,i'} C_{i,j}^* C_{i',j} \langle i'|n'\rangle\langle n|i\rangle = \langle\Psi|\hat{P}_{n',n}|\Psi\rangle , \quad (4)$$

where

$$\hat{P}_{n',n} = \sum_j |j\rangle |n'\rangle \langle n| \langle j| . \quad (5)$$

Instead of a sum over the coefficients of the wave function, one can calculate the elements of the reduced density matrix with the help of expectation values of the operator $\hat{P}_{n',n}$. The effect of $\hat{P}_{n',n}$ is to change the state of the system from $|n\rangle$ to $|n'\rangle$. It can be viewed as a rotation in state space.

After diagonalisation of ρ^{sys} one obtains its eigenvalues ω_α , which define the von Neumann entropy of the system [1,2],

$$S^{\text{sys}} = - \sum_\alpha \omega_\alpha \ln \omega_\alpha . \quad (6)$$

This quantity describes how much the system is entangled with the environment for a given wave function $|\Psi\rangle$. When the basis $\{|n\rangle\}$ describes only one orbital p , then the system contains only this orbital p and the corresponding entropy S^p is the one-orbital entropy. If the system contains two orbitals p, q , then S^{pq} is a two-orbital entropy. Since the two-orbital system is built up from two subsystems, namely, the orbitals p and q , one can apply the subadditivity property of S :

$$S^{pq} \leq S^p + S^q , \quad (7)$$

where the equality holds when p and q are not entangled. The interpretation is straightforward: S^p describes the entanglement of p and S^q the entanglement of q with the rest of the environment, while S^{pq} describes the entanglement of p and q with the rest of the environment. Any entanglement between p and q reduces S^{pq} with respect to the sum of S^p and S^q . Therefore, one can define the entanglement between two individual orbitals by

$$I_{p,q} = \frac{1}{2} (S^p + S^q - S^{pq}) (1 - \delta_{pq}) \geq 0 , \quad (8)$$

where the Kronecker δ ensures that $I_{p,p} = 0$, and the factor 1/2 prevents interactions from being counted twice. The quantity $I_{p,q}$ is interpreted in the remaining part of this work as a measure of the orbital interaction.

Although $I_{p,q}$ describes the entanglement between two orbitals, it is not possible to use $I_{p,q}$ in order to build up entropies of larger systems. For example, when the system contains the orbitals p and the environment the orbitals q , then

$$S^{\text{sys}} > \sum_{p \in \text{sys}, q \in \text{env}} I_{p,q} \quad (9)$$

for all cases that we have investigated. The difference can amount to 60% of S^{sys} .

2.2 A recipe for the calculation S

In order to calculate an orbital interaction using Eq. (8), one has to determine and diagonalise the one- and two-orbital reduced density matrices ρ^p and ρ^{pq} . Their matrix elements are calculated in this work with the help of the right-hand side of Eq. (4), in which the matrix elements are written as expectation values of $\hat{P}_{n',n}$ with respect to the wave function $|\Psi\rangle$, where the operator changes the state of the system from $|n\rangle$ to $|n'\rangle$.

One suitable way to represent the system basis $\{|n\rangle\}$ is the occupation-number representation. In particular, if the system consists of only one orbital p ,

$$\{|n\rangle\} = \{\hat{c}_{p,\uparrow}^\dagger |0\rangle, \hat{c}_{p,\downarrow}^\dagger |0\rangle, |0\rangle, \hat{c}_{p,\uparrow}^\dagger \hat{c}_{p,\downarrow}^\dagger |0\rangle\} = \{|\uparrow\rangle, |\downarrow\rangle, |0\rangle, |\uparrow\downarrow\rangle\} \quad (10)$$

where $\hat{c}_{p,\sigma}^\dagger, \hat{c}_{p,\sigma}$ are creation and annihilation operators for electrons with spin σ in the orbital p , and $|0\rangle$ is the vacuum state. Eq. (10) leads to a one-orbital density matrix of dimension four. If the system contains two orbitals, then $\{|n\rangle\}$ consists of sixteen basis states, where the orbitals p and q are occupied by zero to four electrons

$$\{|n\rangle\} = \{|\uparrow, 0\rangle, |\uparrow, \uparrow\rangle, |\uparrow, \downarrow\rangle, |\uparrow, \uparrow\downarrow\rangle, |\downarrow, \uparrow\downarrow\rangle, \dots, |\uparrow\downarrow, \uparrow\downarrow\rangle\} , \quad (11)$$

which leads to a 16×16 two-orbital density matrix.

This representation determines not only the dimension of the resulting density matrices, but has two additional consequences. The first is that the matrix elements of the reduced density matrix $\rho_{n,n'}^{\text{sys}}$ are zero if $|n\rangle$ and $|n'\rangle$ differ in the number of electrons or in the z-component of the spin, for example

$$\rho_{|\uparrow\rangle, |\uparrow\downarrow\rangle}^p = \sum_j \langle \Psi | j \rangle | \uparrow \downarrow \rangle \langle \uparrow | \langle j | \Psi \rangle = 0 . \quad (12)$$

Since all of the basis states in Eq. (10) differ in either the number of electrons or the z-component of the spin, the one-orbital density matrix is diagonal in this representation, as shown in Table 1. The second consequence of Eqs. (10) and (11) is that the matrix elements $\langle \Psi | \hat{P}_{n',n} | \Psi \rangle$ of Eq. (4) can be expressed using creation and annihilation operators. For example,

$$\begin{aligned} \rho_{|\uparrow, \downarrow\rangle, |0, \uparrow\downarrow\rangle}^{pq} &= \sum_j \langle \Psi | j \rangle | \uparrow, \downarrow \rangle \langle 0, \uparrow\downarrow | \langle j | \Psi \rangle \\ &= \langle \Psi | \hat{c}_{p,\uparrow}^\dagger (1 - \hat{n}_{p,\uparrow}) \cdot \hat{n}_{q,\downarrow} \hat{c}_{q,\uparrow} | \Psi \rangle , \end{aligned} \quad (13)$$

where $\hat{n}_{p,\sigma} = \hat{c}_{p,\sigma}^\dagger \hat{c}_{p,\sigma}$ is the (occupation-)number operator for electrons with spin σ in the orbital p . We exploit this property in order to determine the one- and two-orbital density matrices.

Table 1

The one-orbital density matrix $\rho_{n,n'}^p$ for an orbital p . The states $\{|n\rangle\}$, $\{|n'\rangle\}$ are defined in Eq. (10). The (occupation-)number operator for electrons with spin σ in the orbital p is $\hat{n}_{p,\sigma} = \hat{c}_{p,\sigma}^\dagger \hat{c}_{p,\sigma}$.

$\rho_{n,n'}^p$	$\langle \uparrow $	$\langle \downarrow $	$\langle 0 $	$\langle \uparrow \downarrow $
$\langle \uparrow $	$\langle \hat{n}_{p,\uparrow} (1 - \hat{n}_{p,\downarrow}) \rangle$	0	0	0
$\langle \downarrow $	0	$\langle \hat{n}_{p,\downarrow} (1 - \hat{n}_{p,\uparrow}) \rangle$	0	0
$\langle 0 $	0	0	$\langle (1 - \hat{n}_{p,\downarrow}) (1 - \hat{n}_{p,\uparrow}) \rangle$	0
$\langle \uparrow \downarrow $	0	0	0	$\langle \hat{n}_{p,\downarrow} \hat{n}_{p,\uparrow} \rangle$

Consequently, the eigenvalues of $\rho_{n,n'}^p$ in Table 1 are written in terms of the occupation-number operator. Thus, the resulting one-orbital entropy S^p depends only on the occupancy of the orbital. In particular, $S^p = 0$ when the orbital is fully occupied or empty, and it reaches its maximal value $S_{\max}^p = \ln 4$ when $\langle \hat{n}_{p,\downarrow} \rangle = \langle \hat{n}_{p,\uparrow} \rangle = 0.5$ and $\langle \hat{n}_{p,\downarrow} \hat{n}_{p,\uparrow} \rangle = 0.25$.

In this work, the occupancies of the orbitals are the same for each spin $\langle \hat{n}_{p,\downarrow} \rangle = \langle \hat{n}_{p,\uparrow} \rangle$, and, using the approximation $\langle \hat{n}_{p,\downarrow} \hat{n}_{p,\uparrow} \rangle \approx \langle \hat{n}_{p,\downarrow} \rangle \langle \hat{n}_{p,\uparrow} \rangle$, one gets

$$S^p(n_p) \approx 2 \left[\left(1 - \frac{n_p}{2}\right) \ln \left(1 - \frac{n_p}{2}\right) + \frac{n_p}{2} \ln \frac{n_p}{2} \right], \quad (14)$$

where $n_p = \langle \hat{n}_{p,\downarrow} \rangle + \langle \hat{n}_{p,\uparrow} \rangle$ is the occupancy of orbital p . Thus, $S^p(n_p)$ is a symmetric function of the occupancy in this case: $S^p(n_p) = S^p(2 - n_p)$. We plot therefore the values of S^p found in this work versus the deviation Δn_p of the occupancy from the Hartree-Fock case in Fig. 1. One to six orbitals deviate from the approximation of Eq. (14), depending on the molecule. The deviations occur for $\Delta n_p \geq 0.025$. The largest one-orbital entropy found in this work $S^p \leq 0.31$ is much smaller than the maximal value $S_{\max}^p \approx 1.38$ because the occupancies do not deviate strongly from the Hartree-Fock case and because $\langle \hat{n}_{p,\downarrow} \hat{n}_{p,\uparrow} \rangle \neq \langle \hat{n}_{p,\downarrow} \rangle \langle \hat{n}_{p,\uparrow} \rangle$.

Finally, in this representation it is possible to see that the two-orbital density matrices also contain the information contained in the reduced one-particle density matrix

$$\rho_{p,q}^{\text{one}} = \sum_{\sigma} \langle \Psi | \hat{c}_{p,\sigma}^\dagger \hat{c}_{q,\sigma} | \Psi \rangle \quad (15)$$

and the reduced two-particle density matrix

$$\rho_{p,q}^{\text{two}} = \sum_{\sigma,\sigma'} \langle \Psi | \hat{n}_{p,\sigma} \hat{n}_{q,\sigma'} | \Psi \rangle. \quad (16)$$

The elements of ρ^{one} are contained in the off-diagonal elements of the two-orbital density matrices ρ^{pq} while the elements of ρ^{two} are contained in those diagonal elements of ρ^{pq} where p and q are always occupied.

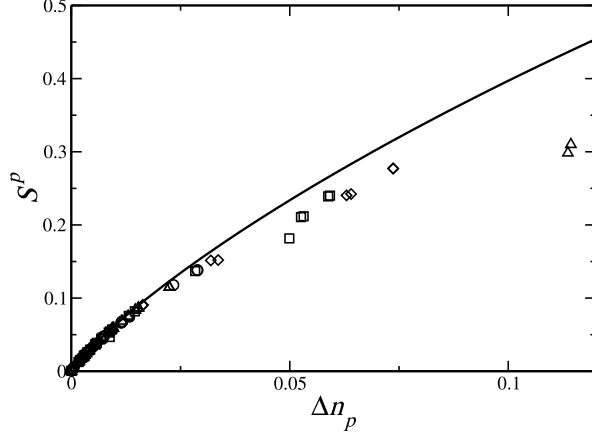


Fig. 1. One-orbital entropy S^p as defined in Eq. (6) and Table 1 versus the deviation of the occupancy of orbital p , $n_p = \langle \hat{n}_{p,\downarrow} \rangle + \langle \hat{n}_{p,\uparrow} \rangle$, from the Hartree-Fock case ($\Delta n_p = 2 - n_p$ if $n_p \geq 1$ and $\Delta n_p = n_p$ if $n_p < 1$): circles - LiF, squares - CO, diamonds - N₂, triangles - F₂. Solid line - Eq. (14). The values of S^p are taken from a DMRG calculation at $m = 200$ and Hartree-Fock ordering.

This leads to the following recipe to calculate the orbital entanglement of Eq. (8):

- (1) Calculate an approximate wave function $|\Psi\rangle$.
- (2) Calculate the one-orbital and two-orbital density matrices ρ^p for every orbital p and q , and ρ^{pq} for every combination p, q .
- (3) Diagonalise the density matrices and calculate the entropies S^p and S^{pq} using the eigenvalues ω_α .
- (4) Calculate $I_{p,q}$.

In order to follow this recipe and to make use of the formulation of Eqs. (4) and (13), it is necessary to apply a method that can easily calculate expectation values of operators in second quantisation with respect to the total wave function. This is the case for the DMRG, which is described in the following section.

3 The DMRG and the calculation of von Neumann entropies

This section presents only those aspects of the DMRG that are relevant for the following discussion. For further details we refer the reader to Refs. [3,7,8].

3.1 The setup

The DMRG is used here to determine the ground state and its energy for the time-independent, non-relativistic, electronic Hamiltonian (Full-CI problem) with a well-defined error. The second-quantised Hamiltonian reads

$$\hat{H} = \sum_{p,q,\sigma} T_{p,q}^{\sigma} \hat{c}_{p,\sigma}^{\dagger} \hat{c}_{q,\sigma} + \sum_{p,q,r,s,\sigma,\sigma'} V_{p,q,r,s}^{\sigma,\sigma'} \hat{c}_{p,\sigma}^{\dagger} \hat{c}_{q,\sigma'}^{\dagger} \hat{c}_{r,\sigma'} \hat{c}_{s,\sigma}. \quad (17)$$

Typically, $T_{p,q}^{\sigma}$, $V_{p,q,r,s}^{\sigma,\sigma'}$ are the one- and two-electron integrals in the basis of the canonical orbitals p, q, r, s , i.e., the eigenfunctions of the Fock-operator.

The determination of *all* of the eigenstates of Eq. (17) requires a diagonalisation in a Hilbert space which grows exponentially with the number of orbitals N : $\dim(\mathcal{H}) = 4^N$. The key idea of the DMRG is to form a reduced basis in an optimal, controlled way for the *few* eigenstates one is interested in, thus reducing the numerical effort. The size of the reduced basis \mathcal{B} in this work is $\dim(\mathcal{B}) = 16 \cdot m^2$.

For a given m , one determines the optimal basis iteratively with the help of the reduced density matrix (Eq. (2)). This requires the formation of a wave function as in Eq. (1) in every step. Consequently, one also must divide the total basis into a “system” and an “environment” part which is realised in the following way: First, one orders the orbitals onto a one-dimensional lattice, see Fig. 2. Second, a boundary line defines a left and a right block. The product states that can be formed with the orbitals of each block are represented in this work by $4m$ states: the states of one block are the “system” states $\{|i\rangle\}$ and the states of the other block are the “environment” states $\{|j\rangle\}$ in Eqs. (1) and (2).

In every step of the algorithm the boundary is moved by one site. When the separator is moved from left to right, the left block plays the role of the “system” and the right block the role of the “environment”. When the separator is moved from right to left the roles are exchanged. A zipper-like motion of the boundary back and forth through the whole lattice is called a sweep.

Finally, it is important to point out that the ordering of the orbitals onto the lattice is in principle arbitrary. One can therefore choose to order the orbitals on the lattice with increasing energy, an ordering which we will call the Hartree-Fock (HF) ordering for the rest of this work. The influence on the energy convergence of different orderings, as mentioned in Section 1, is discussed in Section 5.

In the subsequent sections, the ground states of LiF, CO, N₂, and F₂ are in-

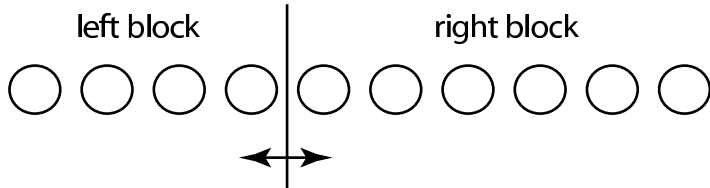


Fig. 2. Setup of the DMRG: every orbital occupies one lattice site. In every step of the DMRG the separator is moved one site to the right or to the left.

investigated. The same cc-pVDZ basis set [9] has been used for all molecules, which gives rise to $N = 28$ canonical orbitals. We have calculated the one- and two-electron integrals using Dalton, a standard quantum-chemistry program package [10]. The molecules have been calculated at their experimental distances: $r_{\text{LiF}} = 156.3864$ pm, $r_{\text{CO}} = 112.8323$ pm, $r_{\text{N}_2} = 109.768$ pm, $r_{\text{F}_2} = 141.193$ pm [11,12,13,14].

3.2 The error in energy and the measurement of $I_{p,q}$

The states $|i\rangle$ of the system block are improved in every step of the algorithm. In particular, one diagonalises the Hamiltonian (Eq. (17)) in the reduced basis \mathcal{B} , calculates the reduced density matrix ρ^{sys} (Eq. (2)) and projects the $4m$ basis states representing the system block onto those m eigenstates of $\rho_{i,i'}^{\text{sys}}$ that have the largest eigenvalues ω_α and are in that sense an optimal representation of the system block. The eigenvalues ω_α also define the projection error of one step of the DMRG

$$P_m^{\text{step}} = 1 - \sum_{\alpha=1}^m \omega_\alpha \quad (18)$$

since $\sum_\alpha \omega_\alpha = 1$. We take the projection error for a given m , P_m , to be P_m^{step} at the step when the separator is in the middle of the lattice in the last sweep, assuming that convergence in the number of sweeps has been achieved.

If m is large enough so that $\dim\mathcal{B} = \dim\mathcal{H}$, then the Full-CI problem is solved and $P_m = 0$. Since the DMRG is variational, every energy for a given m is larger than the exact energy $E_m \geq E_{\text{exact}}$. Therefore, E_m can be extrapolated to the exact (Full-CI) ground state energy E_{exact} , which is in our case unknown, using [5]

$$E_m = E_{\text{exact}} + \alpha P_m . \quad (19)$$

In order to obtain E_{exact} , we calculate a linear regression to $E_m(P_m)$ at six different $m = (200, 300, 400, 500, 600)$. Typically, six sweeps are necessary to obtain a converged energy at $m = 200$ and four additional sweeps for each of the other values of m . Table 4 contains the extrapolated energies E_{exact} . The errors given in Table 4 are the standard deviations for E_{exact} due to the extrapolation procedure, and we use error in this sense for the rest of this manuscript. There are other definitions in the literature for the error in energy

which also depend on P_m^{step} [15] and which consequently should give similar results.

In order to calculate the orbital interaction $I_{p,q}$, one has to form the operators that lead to the reduced one- and two-orbital density matrices using Eqs. (4) and (11). For example, instead of evaluating Eq. (13) as a whole, one determines

$$\rho_{|\uparrow,\downarrow\rangle,|0,\uparrow\downarrow\rangle}^{pq} = \langle \Psi | \hat{c}_{p,\uparrow}^\dagger \cdot \hat{n}_{q,\downarrow} \hat{c}_{q,\uparrow} | \Psi \rangle - \langle \Psi | \hat{c}_{p,\uparrow}^\dagger \hat{n}_{p,\uparrow} \cdot \hat{n}_{q,\downarrow} \hat{c}_{q,\uparrow} | \Psi \rangle . \quad (20)$$

In this way, every matrix element of $\rho_{n,n'}^{pq}$ is expressed as sum of matrix elements of smaller operators. Only 23 of them are needed to construct $\rho_{n,n'}^{pq}$. They are stored in matrix form and must be transformed into the new basis at every step of the DMRG. We evaluate the 23 operators at the end of a DMRG calculation with the wave function $|\Psi\rangle$ from the last step and calculate $\rho_{n,n'}^{pq}$ from the DMRG output.

Although the one-orbital entropies can be determined throughout the DMRG algorithm by calculating the local densities $\langle \hat{n}_{i,\sigma} \rangle$ via Table 1, it is necessary to also calculate them at the end of the procedure in order to obtain comparable accuracy in each matrix element and in order to calculate them with respect to the same wave function as the two-orbital entropies.

4 The structure and accuracy of $I_{p,q}$

We have carried out calculations for the electronic ground state of the four test molecules (LiF, CO, N₂, F₂). We have obtained wave functions with different energies and errors by changing some parameters of the algorithm: the underlying symmetry of the Hartree-Fock calculation, the ordering of the orbitals, and the parameter m . It turns out that the general structure of $I_{p,q}$ is not affected by these parameters. In other words, $I_{p,q}$ can already be determined using a comparatively inexpensive calculation, for example with $m = 200$ at HF ordering in any symmetry.

The values of $I_{p,q}$ are in the range $0 < I_{p,q} < 0.18$ in this work. The maximal values for the different molecules are $I_{p,q} = 0.03$ for LiF, $I_{p,q} = 0.08$ for CO, $I_{p,q} = 0.11$ for N₂, and $I_{p,q} = 0.18$ for F₂. The distribution of the $I_{p,q}$ values is shown in Fig. (3). One can see that LiF, the only molecule in the series with an ionic bond, has a broad distribution of elements, while the other molecules show a somewhat smaller distribution and two or three intervals with a large concentration of $I_{p,q}$ elements. The largest interaction $I_{p,q}$ for F₂ is one order of magnitude larger than the second largest interaction element. Also N₂ and CO have two to three interaction elements that are clearly separated from the

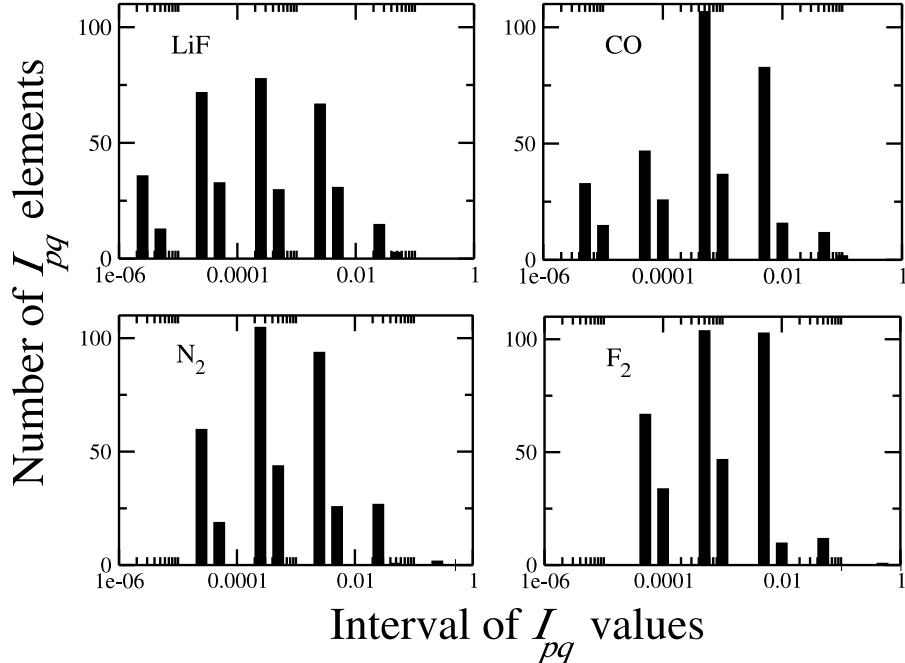


Fig. 3. Histograms of $I_{p,q}$ calculated at HF ordering for $m = 200$: The number of $I_{p,q}$ elements are counted for consecutive intervals. For example, the number of elements in $0.0001 \leq I_{p,q} < 0.0005$ is displayed at 0.0005, the number in $0.0005 \leq I_{p,q} < 0.001$ is displayed at 0.001 and so on.

rest, which is not the case for LiF.

In order to visualise the structure of $I_{p,q}$, it is useful to assign a label to each orbital. In this work, the orbital labels stem from a Hartree-Fock calculation using the highest point group available in the Dalton program package: D_{2h} for F_2 , N_2 and C_{2v} for LiF, and CO. This means that the lowest-lying orbital in F_2 always has the label $1a_g$, even for calculations in C_1 . Using these labels, we can specify the order in which the orbitals are put on the lattice in the DMRG calculation. The orderings are given in Tables 2 and 3, together with a label for the different cases. The labels designate the molecule, the ordering criterion, and the point group in which the HF calculation is carried out. For example, LiF-HF- C_1 denotes a calculation for the LiF molecule, ordering by the orbital energies (HF ordering), and utilising a HF calculation in C_1 .

The structure of $I_{p,q}$ can be examined using diagrams. We connect two orbital labels with a line if the corresponding value for $I_{p,q}$ is larger than a chosen threshold, here $I_{p,q} > 0.005$. In Fig. 4, we display such diagrams for the four molecules studied where the calculations have been carried out using the HF ordering and $m = 200$. From the diagrams, one can see the following features: First, in all cases the interaction couples predominantly orbitals of the same irreducible representation. Second, there are a few orbitals which are also cou-

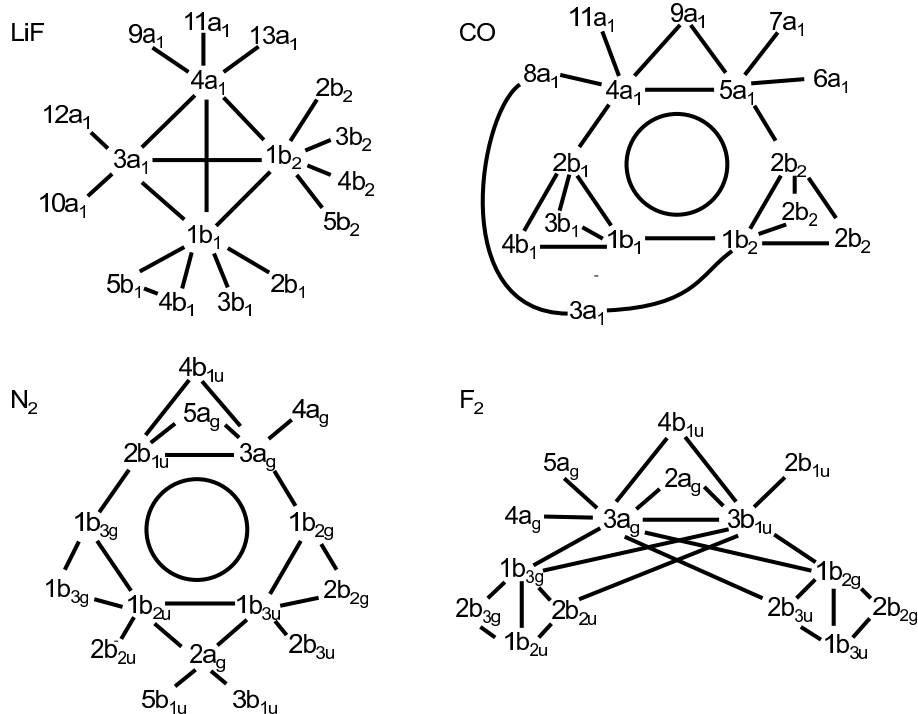


Fig. 4. Diagram of $I_{p,q}$ calculated at HF ordering and $m = 200$: Lines connect orbital labels with $I_{p,q} > 0.01$. The circle for CO and N_2 denotes that the surrounding orbitals are all connected with each other.

pled to orbitals of other irreducible representations (for example $3a_1$, $4a_1$, $1b_1$, $1b_2$ in LiF). Third, those orbitals which couple different symmetry sectors are often energetically close to the highest occupied molecular orbital (HOMO). They have an occupancy n_p that deviates from $n_p = 2$ or $n_p = 0$ and thus have a large one-orbital entropy S^p according to Section 2.

Therefore, one can say that orbitals with a large one-orbital entropy S^p also have large interactions $I_{p,q}$. They are often energetically close to the HOMO and are frontier orbitals in that sense (see Section 1). One can also ask, whether the value $I_{p,q}$ is connected to the integrals $T_{p,q}^\sigma$ and $V_{p,q,r,s}^{\sigma,\sigma'}$ of the Hamiltonian in Eq. (17). To answer this question, we have a look at the largest $I_{p,q}$ which always correspond to orbitals $p - q$ which are $\sigma_z - \sigma_z^*$, $\pi_x - \pi_x^*$, or $\pi_y - \pi_y^*$ combinations. The bonding and anti-bonding orbitals belong to the same irreducible representation for LiF and CO. For F_2 and N_2 , however, these orbitals belong to different irreducible representations. Consequently, $T_{p,q}^\sigma = 0$ for the latter cases and p, q are only connected by two-electron integrals in the Hamiltonian, whereas for LiF and CO one can find one- and two-electron integrals. It is therefore not possible to deduce a clear correspondence between the size of $I_{p,q}$ and the size of the one- and two-electron integrals.

Another way to visualise the overall structure of $I_{p,q}$ is to plot this quantity as a matrix for a given ordering. For example, the element $I_{2,5}$ for case LiF-HF-

C_{2v} denotes the interaction between the $2a_1$ and $1b_1$ orbital. This also makes it possible to mirror the effect of different orderings: an ordering which groups strongly interacting orbitals together has large elements next to the diagonal in the plot of $I_{p,q}$.

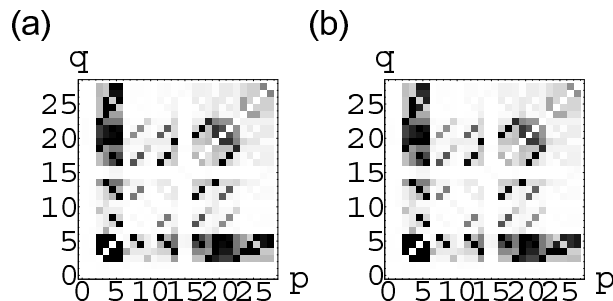


Fig. 5. $I_{p,q}$ calculated for ordering LiF-HF- C_{2v} (label defined in Table 2) with (a) $m = 200$ and (b) $m = 600$.

In Fig. 5, we display plots of $I_{p,q}$ for the case LiF-HF- C_{2v} with $m = 200$ and $m = 600$. The increase in accuracy has no significant effect on $I_{p,q}$, although the electronic energies differ by about $7 \cdot 10^{-3}$ a.u. (see Table 4). It can also be seen that the HF ordering results in large weight in the off-diagonal region of $I_{p,q}$ and thus in an ordering for which strongly interacting orbitals are far apart. This holds also for all other cases of HF ordering.

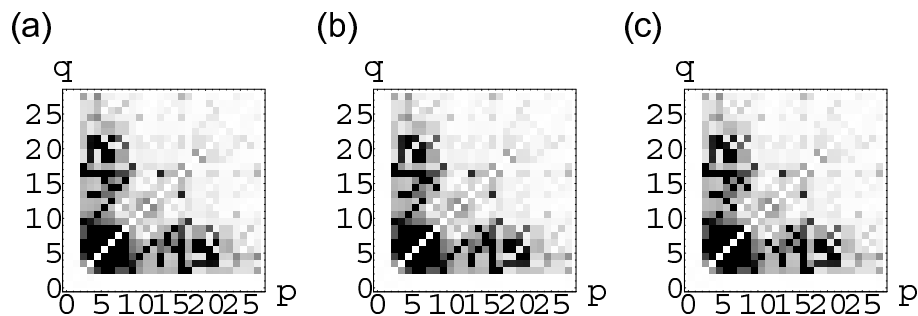


Fig. 6. $I_{p,q}$ calculated for (a) N_2 -HF- D_{2h} and $m = 200$, (b) N_2 -HF- C_{2v} and $m = 600$, and (c) N_2 -HF- C_1 and $m = 600$ (labels defined in Table 3).

In Fig. 6, one can see that the influence on $I_{p,q}$ of different symmetries in the HF calculations is negligible. The plots of $I_{p,q}$ for N_2 and HF ordering in D_{2h} , C_{2v} , and C_1 are almost identical. This is also reflected in Fig. 8 in which the curves of the electronic energies with respect to the DMRG steps lie on top of each other and consequently lead to the same extrapolated energy (see Table 4).

Up to this point, the orbitals have been ordered on the DMRG lattice according to their energy (HF ordering). Different orderings result in different wave functions, energies, and structures of the $I_{p,q}$ matrices. The next section deals with this issue in more detail. For now, only the effect of the different orderings on $I_{p,q}$ is discussed. Fig. 7 shows plots of $I_{p,q}$ for $m = 600$ and three cases from

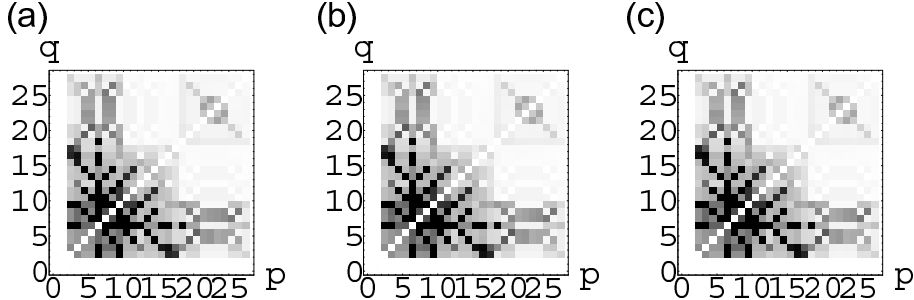


Fig. 7. $I_{p,q}$ from calculation using $m = 600$ and (a) $F_2\text{-HF-}D_{2h}$, (b) $F_2\text{-(23)-}D_{2h}$, and (c) $F_2\text{-[18]-}D_{2h}$ (labels defined in Table 3). The matrices in (b) and (c) are plotted in the HF ordering rather than the ordering of the actual calculation.

Table 3: $F_2\text{-HF-}D_{2h}$, $F_2\text{-(23)-}D_{2h}$, and $F_2\text{-[18]-}D_{2h}$. There is a sizeable energy difference between the HF ordering and the other two cases of approximately $6 \cdot 10^{-3}$ a.u. (see Table 4). Despite these differences, no significant difference in the plots of $I_{p,q}$ is discernible. In order to make this comparison possible, we have plotted all $I_{p,q}$ matrices in the same ordering, namely the HF ordering, although the actual calculations have been carried out using the labelled criteria. In Fig. 13 one can see plots of $I_{p,q}$ for $F_2\text{-(23)-}D_{2h}$ and $F_2\text{-[18]-}D_{2h}$ in the ordering which has been used in the calculation.

To conclude, we find that $I_{p,q}$ is a reliable definition of orbital interaction which can be calculated for small m in any ordering. The next section addresses the question of whether one can use the information in $I_{p,q}$ to obtain an optimal ordering in the sense that the DMRG has a rapid convergence towards the exact wave function and energy.

5 The ordering problem

5.1 The problem and solution strategies

Two things must be chosen before a DMRG calculation can be carried out: the basis and its ordering on the lattice. In principle, any orthonormal basis of orbitals can be used and the ordering is arbitrary. However, the ordering does affect the convergence of the DMRG in practice [4]. This can be seen by analyzing the behaviour of the energies as m is increased. With increasing m , the variational nature of the DMRG leads to a decrease in energy for every ordering. For a sufficiently large m , the difference to the exact energy can be made arbitrarily small. In this sense the ordering is arbitrary. However, the value of m that is necessary for a certain accuracy in energy depends on the ordering. For example, in Fig. 8 one can see that the case $\text{LiF-(23)-}C_{2v}$ leads to a much lower energy for $m = 200$ than $\text{LiF-HF-}C_{2v}$. With increasing m

Table 2

LiF, CO: Orderings of the orbitals as used in the DMRG: The labelling has the form ⟨molecule⟩-⟨ordering criterion⟩-⟨point group⟩ where ⟨molecule⟩ is LiF or CO, ⟨ordering criterion⟩ is HF (increasing orbital energy), (23) (using Eqs. (8), (21), (23)), or [18] (Ref. [18]). The label ⟨point group⟩ is the corresponding Schönflies symbol (for example C_{2v}). Orbital labels stem from calculations at the highest possible point group (here C_{2v}). Occupied orbitals are printed in **bold face**.

Label	Ordering
LiF-HF- C_{2v}	[1a₁ 2a₁ 3a₁ 4a₁ 1b₁ 1b₂ 5a ₁ 2b ₂ 2b ₁ 6a ₁ 7a ₁ 3b ₁ 3b ₂ 8a ₁ 9a ₁ 1a ₂ 4b ₁ 4b ₂ 10a ₁ 11a ₁ 5b ₁ 5b ₂ 12a ₁ 13a ₁ 6b ₂ 6b ₁ 14a ₁ 2a ₂]
LiF-(23)- C_{2v}	[2b ₁ 3b ₁ 4b ₁ 1b₁ 5b ₁ 14a ₁ 2a ₂ 6b ₁ 13a ₁ 6b ₂ 5a ₁ 8a ₁ 4a₁ 11a ₁ 12a ₁ 3a₁ 10a ₁ 6a ₁ 1a₁ 1a ₂ 9a ₁ 2a₁ 7a ₁ 2b ₂ 3b ₂ 4b ₂ 1b₂ 5b ₂]
LiF-[18]- C_{2v}	[1a₁ 2a₁ 9a ₁ 7a ₁ 5a ₁ 6a ₁ 14a ₁ 13a ₁ 10a ₁ 12a ₁ 8a ₁ 3a₁ 11a ₁ 4a₁ 2b ₁ 6b ₁ 3b ₁ 4b ₁ 5b ₁ 1b₁ 1b₂ 5b ₂ 4b ₂ 3b ₂ 6b ₂ 2b ₂ 1a ₂ 1a ₂]
CO-HF- C_{2v}	[1a₁ 2a₁ 3a₁ 4a₁ 1b₁ 1b₂ 5a₁ 2b ₁ 2b ₂ 6a ₁ 3b ₂ 3b ₁ 7a ₁ 8a ₁ 9a ₁ 4b ₂ 4b ₁ 1a ₂ 10a ₁ 5b ₁ 5b ₂ 11a ₁ 12a ₁ 13a ₁ 2a ₂ 6b ₂ 6b ₁ 14a ₁]
CO-(23)- C_{2v}	[5b ₁ 4b ₁ 1b₁ 2b ₁ 5a₁ 7a ₁ 3b ₁ 1a ₂ 6b ₁ 2a₁ 14a ₁ 11a ₁ 9a ₁ 4a₁ 8a ₁ 3a₁ 12a ₁ 6a ₁ 1a₁ 2a ₂ 13a ₁ 6b ₂ 5b ₂ 4b ₂ 1b₂ 2b ₂ 3b ₂ 10a ₁]
CO-[18]- C_{2v}	[1a₁ 2a₁ 14a ₁ 13a ₁ 10a ₁ 12a ₁ 11a ₁ 6a ₁ 7a ₁ 8a ₁ 9a ₁ 3a₁ 4a₁ 5a₁ 6b ₂ 5b ₂ 3b ₂ 4b ₂ 2b ₂ 1b₂ 1b₁ 2b ₁ 4b ₁ 3b ₁ 5b ₁ 6b ₁ 1a ₂ 2a ₂]

the energies for LiF-HF- C_{2v} improve and for $m = 600$ both cases show only a difference in energy of $3 \cdot 10^{-4}$ a.u., as seen in Table 4. However, the error in the energy in Table 4 is considerably larger for LiF-HF- C_{2v} . In the worst case, it is also possible to find orderings that cause a trapping of the DMRG algorithm in a local minimum [4]. The energy then does not decrease significantly with increasing m even though P_m remains small. It is important to note that this trapping is not necessarily due to a certain ordering but is sometimes caused by an unfavourable choice of parameters for the DMRG calculation.

In order to apply the DMRG to practical situations, it is therefore crucial to define a criterion for an optimal ordering for a given basis, in order to avoid trapping in local minima and in order to achieve the highest possible accuracy. The approaches which have been pursued so far have defined an orbital interaction and have ordered the orbitals so that strongly interacting orbitals are near each other on the one-dimensional lattice.

One approach is to define the interaction between orbitals p and q in terms of the one- and two-electron integrals of the Hamiltonian [5,16]. Improved orderings then reduce the bandwidth of the $T_{p,q}^\sigma$ matrix, for example. This approach is not able to avoid trapping in local minima [4]. In order to find an

Table 3

N₂ Orderings of the orbitals as used in the DMRG: The labelling has the form ⟨molecule⟩-⟨ordering criterion⟩-⟨point group⟩ where ⟨molecule⟩ is N₂ or F₂, ⟨ordering criterion⟩ is HF (increasing orbital energy), (23) (using Eqs. (8), (21), (23)), or [18] (Ref. [18]). The label ⟨point group⟩ is the corresponding Schönflies symbol (for example C_{2v}). Orbital labels stem from calculations at the highest possible point group (here D_{2h}). Occupied orbitals are printed in **bold face**.

Label	Ordering
N ₂ -HF- C_1	[1a_g 1b_{1u} 2a_g 2b_{1u} 3a_g 1b_{3u} 1b_{2u} 1b _{3g} 1b _{2g} 3b _{1u} 4a _g 2b _{3u} 2b _{2u} 5a _g $\sim C_{2v}, D_{2h}$ 2b _{3g} 2b _{2g} 4b _{1u} 5b _{1u} 6a _g 1b _{1g} 3b _{3u} 3b _{2u} 6b _{1u} 1a _u 7a _g 3b _{3g} 3b _{2g} 7b _{1u}]
N ₂ -(23)- D_{2h}	[6a _g 1b _{1g} 2b _{2g} 1b _{2g} 1b_{3u} 2b _{3u} 3b _{3u} 1a _u 1a_g 7b _{1u} 3b _{2u} 5a _g 2b_{1u} 3a_g 4b _{1u} 2a_g 5b _{1u} 3b _{1u} 3b _{2g} 1b_{1u} 3b _{3g} 7a _g 4a _g 2b _{2u} 1b_{2u} 1b _{3g} 2b _{3g} 6b _{1u}]
N ₂ -[18]- D_{2h}	[1a_g 7a _g 6a _g 4a _g 5a _g 2a_g 3a_g 1a _u 3b _{3g} 2b _{3g} 1b _{3g} 1b _{2g} 2b _{2g} 3b _{2g} 3b _{2u} 2b _{2u} 1b_{2u} 1b_{3u} 2b _{3u} 3b _{3u} 1b _{1g} 2b_{1u} 4b _{1u} 3b _{1u} 5b _{1u} 6b _{1u} 7b _{1u} 1b_{1u}]
N ₂ -[18]- C_{2v}	[1a_g 1b_{1u} 7b _{1u} 6b _{1u} 7a _g 5b _{1u} 6a _g 4a _g 3b _{1u} 5a _g 4b _{1u} 2a_g 3a_g 2b_{1u} 3b _{2g} 3b _{2u} 2b _{3u} 2b _{3g} 1b _{2g} 1b_{3u} 1b_{2u} 1b _{3g} 2b _{2g} 2b _{2u} 3b _{3u} 3b _{3g} 1b _{1g} 1a _u]
N ₂ -[18]- C_1	[1b_{1u} 3b _{2g} 6b _{1u} 7a _g 1b _{1g} 3b _{2u} 2b _{2u} 3b _{1u} 2b _{3g} 5a _g 2a_g 2b_{1u} 1b _{3g} 1b_{2u} 1b_{3u} 1b _{2g} 3a_g 4b _{1u} 2b _{2g} 2b _{3u} 4a _g 3b _{3u} 6a _g 5b _{1u} 1a _u 7b _{1u} 3b _{3g} 1a_g]
F ₂ -HF- D_{2h}	[1a_g 1b_{1u} 2a_g 2b_{1u} 1b_{2u} 1b_{3u} 3a_g 1b_{2g} 1b_{3g} 3b _{1u} 2b _{3u} 2b _{2u} 4b _{1u} 2b _{2g} 2b _{3g} 4a _g 5a _g 5b _{1u} 6a _g 3b _{2u} 3b _{3u} 7a _g 1b _{1g} 6b _{1u} 1a _u 3b _{2g} 3b _{3g} 7b _{1u}]
F ₂ -(23)- D_{2h}	[5a _g 2b_{1u} 4a _g 3a_g 3b _{1u} 4b _{1u} 6a _g 1b_{1u} 1a_g 3b _{3g} 3b _{2u} 2b _{3g} 1b_{3g} 2b _{2u} 1b_{2u} 2a_g 5b _{1u} 7b _{1u} 6b _{1u} 7a _g 1b _{1g} 1a _u 3b _{2g} 3b _{3u} 1b_{3u} 2b _{3u} 1b_{2g} 2b _{2g}]
F ₂ -[18]- D_{2h}	[1a_g 7a _g 6a _g 5a _g 4a _g 2a_g 3a_g 3b _{1u} 2b_{1u} 4b _{1u} 5b _{1u} 6b _{1u} 7b _{1u} 1b_{1u} 3b _{2g} 2b _{2g} 1b_{2g} 1b_{3g} 2b _{3g} 3b _{3g} 3b _{3u} 2b _{3u} 1b_{3u} 1b_{2u} 2b _{2u} 3b _{2u} 1b _{1g} 1a _u]

ordering criterion based on $T_{p,q}^\sigma$ or $V_{i,j,i,j}^{\sigma,\sigma'}$, a recent study [17] has investigated a large number of orderings for the Cr₂ molecule using a genetic algorithm, which has not yet led to a general criterion for different molecules and basis sets.

Another approach is to group the orbitals according to their irreducible representations and then order the orbitals within these groups in order to maximise the one-orbital entropy S^p along the lattice [4,18]. The net effect is that some entangled (interacting) orbitals are placed close together but are also somewhat distributed over the lattice. This is called “competition between entanglement localisation and interaction localisation” in Ref. [18]. The label “[18]” is attributed to this criterion, which obviously depends on the underlying symmetry of the HF calculation. This is illustrated for N₂-[18]- D_{2h} , N₂-[18]- C_{2v} , and N₂-[18]- C_1 in Fig. 9. The distribution of S^p along the lattice is plotted for

Table 4

Energies and errors due to different orderings: Label - ⟨molecule⟩-⟨ordering criterion⟩-⟨point group⟩ defined in Tables 2 and 3; m - size of the largest used Hilbert space $\dim(\mathcal{B}) = 16 \cdot m^2$; energies - electronic energy in atomic units (without nuclei interaction), extrapolation according to Eq. (19) for $m = 200, 300, 400, 500, 600$ error is the standard deviation.

Label	m	last sweep energy	extrapolated energy (error)
LiF-HF- C_{2v}	200	-116.2870771	
LiF-HF- C_{2v}	600	-116.2936058	-116.2938841 ($\pm 2 \cdot 10^{-4}$)
LiF-(23)- C_{2v}	600	-116.2939879	-116.2940038 ($\pm 2 \cdot 10^{-5}$)
LiF-[18]- C_{2v}	600	-116.2940057	-116.2940214 ($\pm 4 \cdot 10^{-6}$)
CO-HF- C_{2v}	600	-135.5668011	-135.5694985 ($\pm 6 \cdot 10^{-4}$)
CO-(23)- C_{2v}	600	-135.5697747	-135.5711334 ($\pm 7 \cdot 10^{-4}$)
CO-[18]- C_{2v}	600	-135.5703675	-135.5709141 ($\pm 1 \cdot 10^{-4}$)
N ₂ -HF- D_{2h}	600	-132.8983153	-132.9015018 ($\pm 3 \cdot 10^{-4}$)
N ₂ -HF- C_{2v}	600	-132.8983171	-132.9013120 ($\pm 4 \cdot 10^{-4}$)
N ₂ -HF- C_1	600	-132.8983197	-132.9014066 ($\pm 3 \cdot 10^{-4}$)
N ₂ -(23)- D_{2h}	600	-132.9004719	-132.9025150 ($\pm 2 \cdot 10^{-4}$)
N ₂ -[18]- D_{2h}	600	-132.8979579	-132.9006192 ($\pm 2 \cdot 10^{-4}$)
N ₂ -[18]- C_{2v}	600	-132.9020805	-132.9027983 ($\pm 4 \cdot 10^{-5}$)
N ₂ -[18]- C_1	600	-132.8966134	-132.9028483 ($\pm 2 \cdot 10^{-4}$)
F ₂ -HF- D_{2h}	600	-229.4522256	-229.4592938 ($\pm 1 \cdot 10^{-3}$)
F ₂ -(23)- D_{2h}	600	-229.4586797	-229.4615548 ($\pm 2 \cdot 10^{-4}$)
F ₂ -[18]- D_{2h}	600	-229.4581772	-229.4611454 ($\pm 2 \cdot 10^{-4}$)

the three point groups investigated. The maxima correspond to boundaries between groups of orbitals with the same irreducible representation. For the C_1 ordering in Fig. 9(a), the sites with large one-orbital entropy are bunched up in the middle of the lattice. In Fig. 8, we display the effect of these orderings on the convergence of the DMRG: only in the case N₂-[18]- C_{2v} can one see an improvement over the HF ordering N₂-HF- D_{2h} . Therefore, one is not guaranteed that a new ordering according to the strategy of Ref. [18] leads to improved energy convergence.

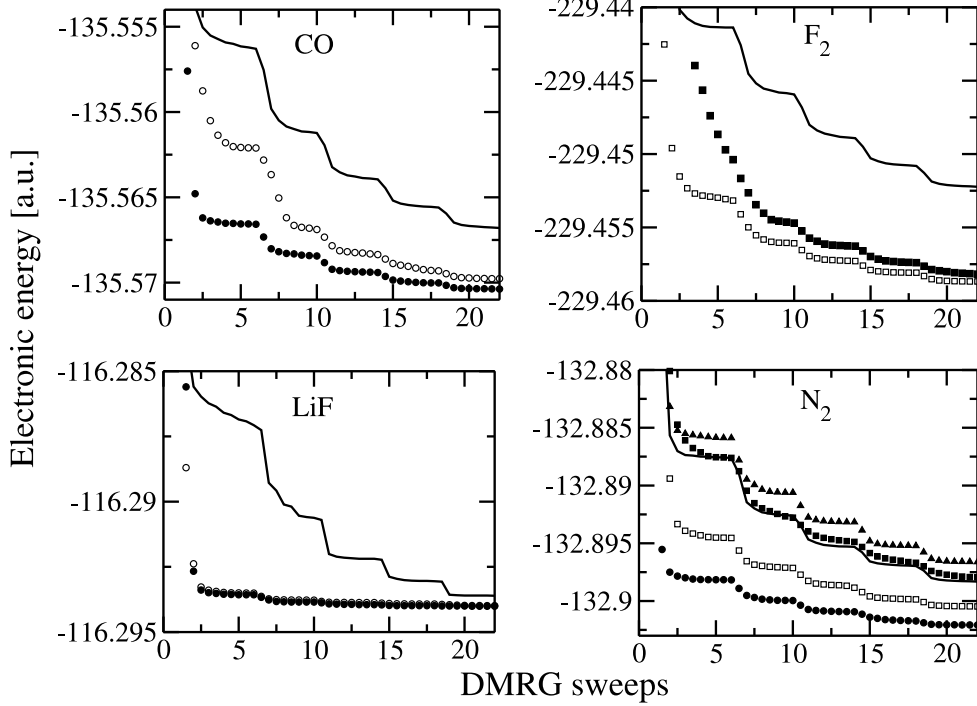


Fig. 8. Electronic energy (no nucleus-nucleus interaction) versus number of DMRG sweeps: $m = 200$ (sweeps 1 to 6), $m = 300$ (sweeps 7 to 10), $m = 400$ (sweeps 11 to 14), $m = 500$ (sweeps 15 to 18), $m = 600$ (sweeps 19 to 22): solid line - HF ordering; open symbols - ordering using Eqs. (8), (21), (23); filled symbols - ordering using Ref. [18]; circles - C_{2v} ; squares - D_{2h} ; triangles - C_1

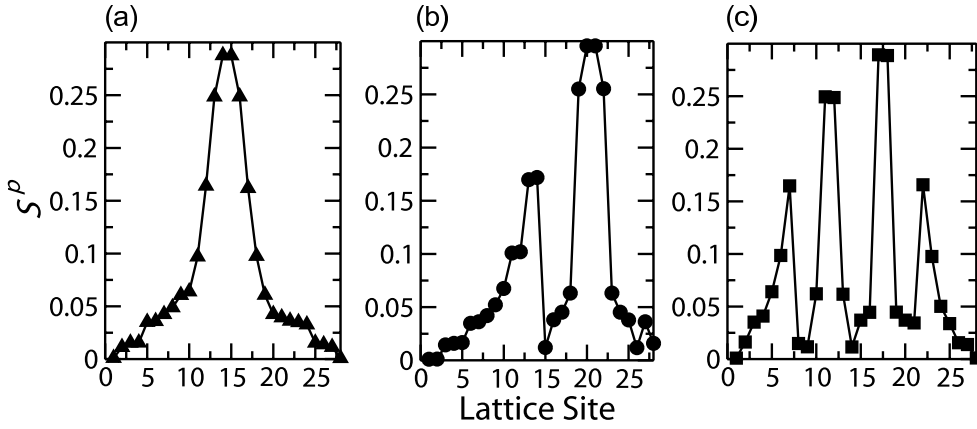


Fig. 9. Orbital entropies S^p following Eq. (6) and Table 1 for (a) N₂-[18]- C_1 , (b) N₂-[18]- C_{2v} , and (c) N₂-[18]- D_{2h} (labels defined in Table 3).

5.2 New strategy using $I_{p,q}$

A strategy based on the orbital interaction $I_{p,q}$ combines the advantages of the two earlier approaches. On the one hand, one is using the entanglement

information of a many-body wave function as in Ref. [18]. On the other hand, one has a specific interaction in matrix form as in Refs. [5,16,17]. The quantity S^p is not sufficiently specific because it only indicates how much orbital p interacts with all the other orbitals, while $I_{p,q}$ is a direct measure of the interaction between p and q . The analysis of $I_{p,q}$ in Fig. 4 has also shown that orbitals from the same irreducible representation are coupled strongly. It is therefore not necessary to account for this fact separately as had to be done in Ref. [18].

Here we search for an improved ordering which localises the interaction $I_{p,q}$, i.e., reduces the bandwidth of the $I_{p,q}$ matrix. The optimal ordering is found using simulated annealing [19]. We argue that this approach is an improvement over the Cuthill-McKee algorithm, used for example in Refs. [5,16], which distinguishes only between occupied and unoccupied matrix elements and thus neglects the information contained in the size of the elements. The annealing algorithm is comparable to the genetic algorithm [17] because both probe different, randomly generated configurations. The cost function in the annealing process plays a similar role to the fitness function in the genetic algorithm.

Following the idea that good orderings should place strongly interacting orbitals near each other, we have investigated several cost functions F that all favour orderings in which large elements of $I_{p,q}$ are on the secondary diagonal and which have a small bandwidth. It turns out that a cost function

$$F = \frac{I_{p,q}}{r^2}, \quad (21)$$

where $r = |p - q|$, is a good starting point. In order to increase the attraction to the secondary diagonal of large elements of $I_{p,q}$, we set

$$r = \begin{cases} 0.5 & \text{if } |p - q| = 1 \\ |p - q| & \text{otherwise.} \end{cases} \quad (22)$$

We have also made further adjustments to the cost function F . From the discussion of the ordering criterion in Ref. [18], we have learned that strongly interacting orbitals should not be bunched up, (for example, in the middle of the lattice) but should instead be more evenly distributed. Therefore, we set $r = 0.5$ for elements on the secondary diagonal in regions of length $N/5$ around the edges and the middle of the lattice, where N is the number of orbitals, i.e.,

$$r = \begin{cases} 0.5 & \text{if } |p - q| = 1 \text{ and} \\ & (\{p, q\} \leq N/5 \text{ or } \{p, q\} \geq N - N/5 \text{ or} \\ & N/2 - N/10 \leq \{p, q\} \leq N/2 + N/10) \\ |p - q| & \text{otherwise.} \end{cases} \quad (23)$$

An ordering created by the use of Eqs. (8), (21) and (23) will be labelled “(23)”.

In all cases in which orderings have been generated using Eq. (23) we have found an improved energy convergence with respect to calculations with HF ordering, and the calculations are not trapped. However, we find that there is no clear correspondence between the value of the cost function for a given ordering and the respective energy convergence. In other words, small changes in the ordering and the cost function can influence the energy convergence severely. For example, the case LiF-[18]- D_{2h} has a similar energy convergence as the case LiF-(23)- D_{2h} as shown in Table 4. However, $F = 0.6397$ in the former case and $F = 1.574$ in the latter, while the HF ordering yields $F = 0.281$.

To summarize, while, in our opinion, Eqs. (21) and (23) represent an improved cost function, one cannot always be certain that an ordering determined by these equations really is the optimal one. While the value of F contains valuable information, additional information, which can be obtained by the visual investigation of $I_{p,q}$ as a matrix, is also important. This will be discussed for specific cases in the following.

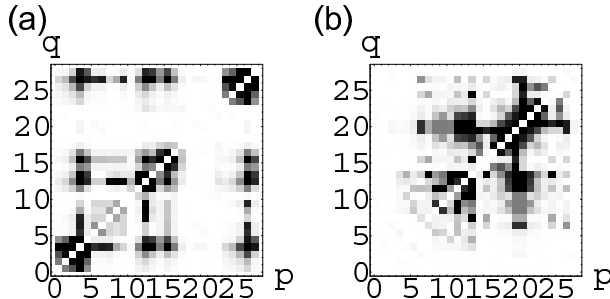


Fig. 10. $I_{p,q}$ calculated at $m = 600$ for (a) LiF-(23)- C_{2v} , and (b) LiF-[18]- C_{2v} (labels defined in Table 2).

LiF, for example, is a rather unproblematic case: any new ordering that reduces the bandwidth of $I_{p,q}$ results in improved convergence in the DMRG. In Fig. 10(a), one can see that the bandwidth of $I_{p,q}$ for the ordering of this work is reduced compared to the HF ordering, which results in a reduced extrapolated energy and a reduced error (see Table 4 and Fig. 8). While the result using the criterion of Ref. [18] looks more compact (Fig. 10(b)), it yields similar results for the energy convergence. A comparison of the orbital orderings in Table 2 shows that both cases group together orbitals of the same irreducible representation.

For CO and N_2 , the situation is more complicated. In Fig. 11(a), one can see that the form of $I_{p,q}$ for our ordering is again more spread out than for the ordering of Ref. [18] (Fig. 11(b)). This time, however, the latter criterion leads to a more exact energy, as can be seen in Fig. 8.

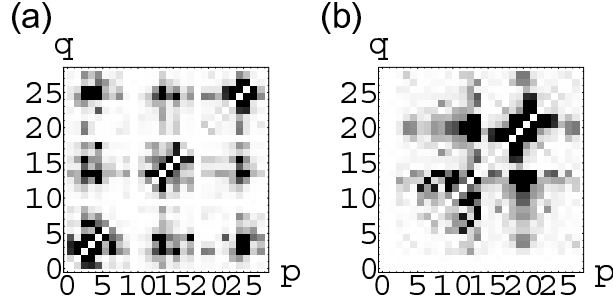


Fig. 11. $I_{p,q}$ calculated at $m = 600$ for (a) CO(23)- C_{2v} , and (b) CO-[18]- C_{2v} (labels defined in Table 2).

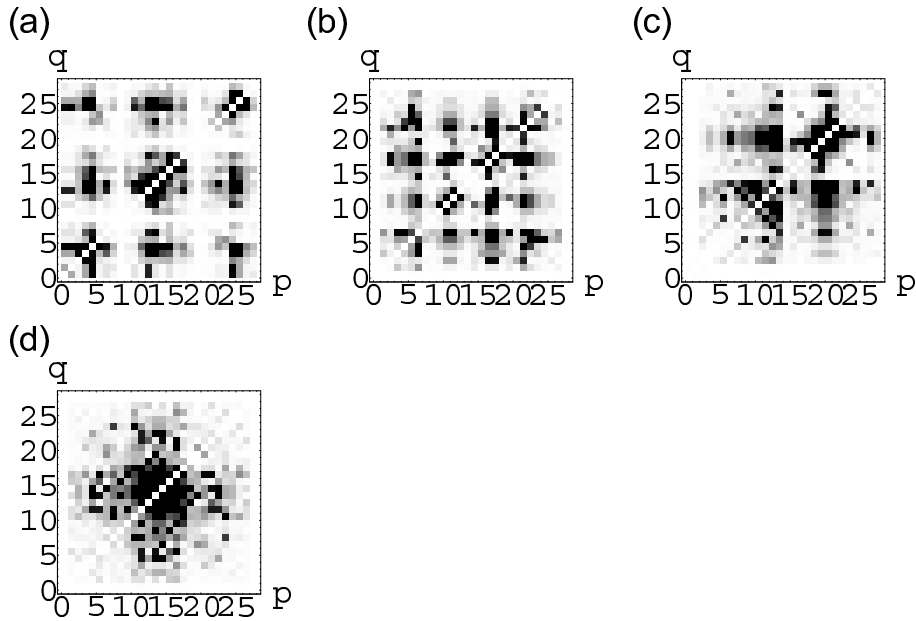


Fig. 12. $I_{p,q}$ calculated at $m = 600$ for (a) N_2 -(23)- D_{2h} , (b) N_2 -[18]- D_{2h} , (c) N_2 -[18]- C_{2v} , and (d) N_2 -[18]- C_1 (labels defined in Table 3).

Fig. 12(a) shows $I_{p,q}$ for N_2 plotted for the ordering criterion of this work. Figs. 12(b)-(d) are determined by the criterion of Ref. [18] and use different symmetries in the underlying HF calculation. All four plots have a reduced bandwidth compared to the HF ordering shown in Fig. 6, but only the cases in Figs. 12(a) and 12(c) show better energy convergence. The criterion of Ref. [18] yields a slightly more compact form of $I_{p,q}$, as can be seen in Fig. 12(c), and leads to a better convergence in energy than our criterion (see Fig. 8). The cases displayed in Figs. 12(b) and 12(d) distribute or accumulate the interacting orbitals too much, leading to poor energy convergence, as explained in the discussion of Fig. 9. This underscores that subtle changes in the structure of the $I_{p,q}$ matrix influence the energy convergence of the DMRG.

For F_2 , in Fig. 13 one cannot say that one plot of $I_{p,q}$ is more compact than the other. Despite this similarity, the differences in the energy convergence are

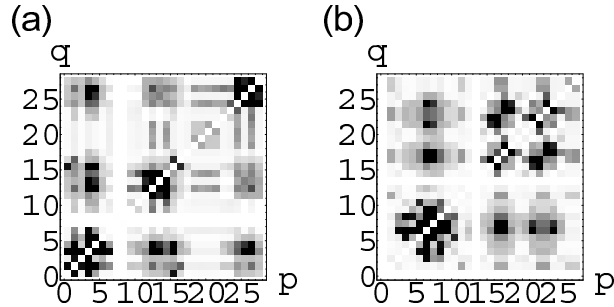


Fig. 13. $I_{p,q}$ calculated at $m = 600$ for (a) F_2 -(23)- D_{2h} and (b) F_2 -[18]- D_{2h} (labels defined in Table 3).

as pronounced as for CO. Only this time the criterion of our work leads to the more exact energy.

To conclude, we can say that the application of $I_{p,q}$, Eqs. (21) and (23) leads to an ordering with a considerably better energy convergence than a HF ordering, and the results do not depend on the symmetry used for the underlying HF calculation. In addition, orderings with a good energy convergence have the following properties: the bandwidth of the $I_{p,q}$ matrix is small, large elements $I_{p,q}$ are grouped on the secondary diagonal, and pronounced accumulation and scattering of large $I_{p,q}$ elements are avoided.

However, we have not been able to establish a distinct correspondence between the orbital interaction and the energy convergence, although $I_{p,q}$ is a very reliable quantity. Therefore, one should test a few different orderings determined by varying some of the parameters of the annealing process before one sets up a DMRG calculation aimed at high accuracy. The resulting energy convergence can be checked for small sizes of the Hilbert space. This is demonstrated in Fig. 8, where the orderings with the lowest energy for $m = 200$ also have the lowest energy for $m = 600$.

5.3 Change of the basis

Evidently, it is desirable to obtain additional insight into the mechanism for energetic convergence in the DMRG. One way to achieve this is not only to consider the ordering of the orbitals but also the choice of the orbitals themselves. Since the canonical orbitals are not a mandatory choice, it is possible to construct a new basis that might suit the DMRG better. So far, there has been one attempt to use a localised basis in the DMRG [20] that has not, however, led to an improved convergence relative to canonical orbitals.

An obvious choice are natural orbitals, i.e., the eigenfunctions of the one-particle density matrix (Eq. (15)). They lead to rapid convergence of the

configuration interaction scheme, and should therefore be favourable for the DMRG as well. Since the one-particle density matrix is contained in ρ^{pq} , one can easily construct approximate natural orbitals, for example, from an approximate wave function of a calculation at $m = 200$ with HF ordering.

The natural orbitals must also be ordered on the lattice. One can use an ordering according to occupation number as a reference ordering. DMRG results for the electronic energies for the four sample molecules calculated with canonical and natural orbitals for various orderings are displayed in Fig. 14. One can see that there is a small increase in convergence for the natural orbitals compared to the canonical orbitals in the HF ordering in every case. One can then apply the ordering criterion of this work which consistently improves energy convergence. However, the optimal energy convergence does not exceed that found for the best orderings of canonical orbitals (not shown in Fig. 14).

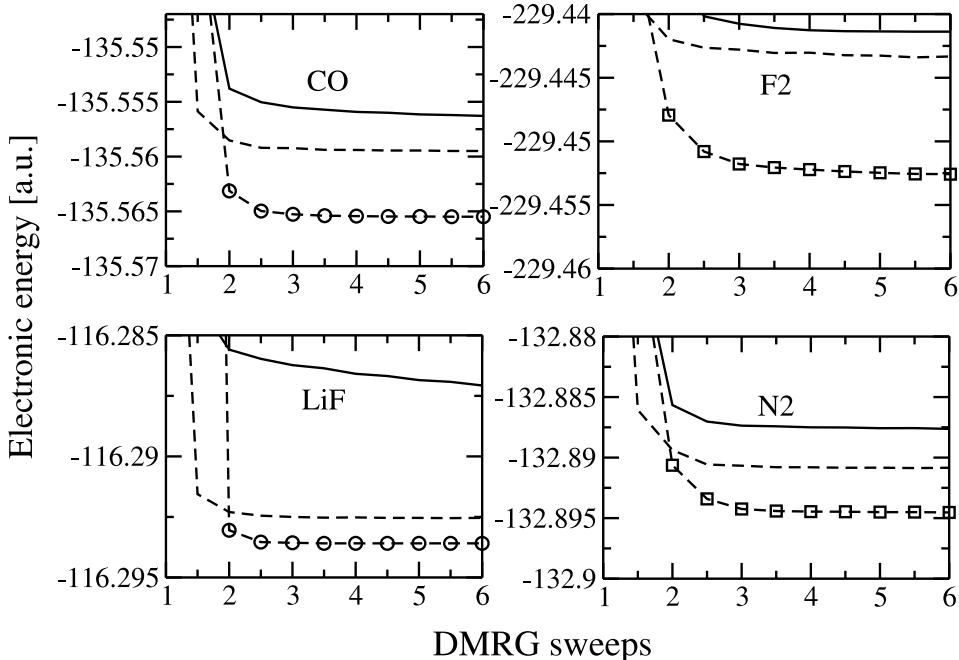


Fig. 14. Electronic energies (no nucleus-nucleus interaction) versus number of DMRG sweeps for $m = 200$ (sweeps 1 to 6). Solid line: canonical orbitals and HF ordering, dashed line: natural orbitals ordering by eigenvalues, dashed line (circles, squares): natural orbitals ordering with Eqs. (8), (21), (23) (C_{2v} , D_{2h}).

Finally, one can consider an iterative improvement of the natural orbitals: Beginning with a DMRG calculation using canonical orbitals in HF ordering, one can obtain an improved wave function which can then be used to calculate natural orbitals which in turn can serve as a basis for a next DMRG calculation yielding a wave function with an even lower energy. This procedure can be repeated yielding an improved wave function and energy at every iteration until the energy converges. We have applied this iterative procedure and have

found that the energies decrease only for two or three iterations and then start to fluctuate. Therefore, further investigation is needed to understand how to construct an optimal basis for the DMRG.

6 Summary

In this work, we have used concepts from quantum information theory to formulate a definition of orbital interaction $I_{p,q}$. For a given wave function, $I_{p,q}$ is defined by the subtraction of the entanglement of two orbitals taken together with the rest of the system from the sum of the entanglement of two individual orbitals with the rest of the system. The advantage of this definition is that one includes information beyond the Hartree-Fock treatment. The disadvantage is that a correlated wave function must be calculated. Given a correlated wave function, we have developed a recipe in Section 2.2 for the calculation of $I_{p,q}$. This recipe additionally provides an alternative method to calculate one-orbital entropies which are also of central importance in other work [4,18].

We have calculated $I_{p,q}$ using correlated wave functions obtained from a DMRG calculation and the recipe of Section 2.2. The resulting interaction $I_{p,q}$ does not depend strongly on the accuracy of the underlying wave function. For the four test molecules we have treated, we have shown that it is possible to calculate $I_{p,q}$ in a reliable fashion. The structure of $I_{p,q}$ is consistent with another criterion based on one-orbital entropies and with chemical intuition: partially occupied orbitals of the same irreducible representation interact strongly.

As an application, we have used $I_{p,q}$ to study the ordering problem in the DMRG, in which one has to order orbitals on a one-dimensional lattice so that strongly interacting orbitals are near each other. We have developed a cost function for a simulated annealing process that leads to an improved ordering for all of the cases we have treated, i.e., the subsequent DMRG calculation leads to a lower energy. We have also found that orderings with a good energy convergence have a small bandwidth in the $I_{p,q}$ matrix, and have a distribution of large matrix elements on the secondary diagonal that is relatively uniform along the lattice. However, we have not been able to identify a consistent scheme that leads to an optimal ordering of the orbitals for the DMRG with this approach. Careful checks and additional attempts to find better orderings are needed.

A more general solution to this problem might lie in the construction of the basis itself. We have therefore investigated the influence of the use of natural orbitals on the convergence of the DMRG. This leads to a slight improvement over the use of canonical orbitals, but the ordering problem still remains. It

is known, however, that the DMRG yields excellent results with a basis of p_z orbitals for conjugated polymers. Hence, an optimal basis should consist of orbitals that are localised in real space and are close in energy. It might then be possible to construct an optimal basis for the DMRG for which the ordering is either obvious or irrelevant. Then the ordering problem should be of minor importance. This will be the topic of a subsequent study.

Acknowledgements

J. Rissler acknowledges the support by the Alexander von Humboldt Foundation.

References

- [1] A. Peres, Quantum Theory: Concepts and Methods, in: Fundamental Theory of Physics, Kluwer, Dordrecht, 1995.
- [2] J. Preskill, Lecture notes, <http://www.theory.caltech.edu/people/preskill/ph229/#lecture>.
- [3] S.R. White, Phys. Rev. Lett. 69 (1992) 2863; Phys. Rev. B 48 (1993) 10345.
- [4] Ö. Legeza, J. Sólyom, Phys. Rev. B 68 (2003) 195116.
- [5] G. K.-L. Chan, M. Head-Gordon, J. Chem. Phys. 116 (2002) 4462.
- [6] R.P Feynman, Statistical Mechanics - a Set of Lectures, in: Frontiers in Physics, D. Pines (Ed.), Reading, Massachusetts, 1972.
- [7] I. Peschel, X. Wang, M. Kaulke, K. Halberg (Eds.), Density-Matrix Renormalization Group, A New Numerical Method in Physics, Lecture Notes in Physics 258, Springer, Berlin, 1999.
- [8] U. Schollwöck, Rev. Mod. Phys. 77 (2005) 259.
- [9] T.H. Dunning, Jr. J. Chem. Phys. 90 (1989) 1007.
- [10] “DALTON, a molecular electronic structure program, Release 1.2 (2001)”, written by T. Helgaker, H. J. Aa. Jensen, P. Jørgensen, J. Olsen, K. Ruud, H. Ågren, A. A. Auer, K. L. Bak, V. Bakken, O. Christiansen, S. Coriani, P. Dahle, E. K. Dalskov, T. Enevoldsen, B. Fernandez, C. Hättig, K. Hald, A. Halkier, H. Heiberg, H. Hettema, D. Jonsson, S. Kirpekar, R. Kobayashi, H. Koch, K. V. Mikkelsen, P. Norman, M. J. Packer, T. B. Pedersen, T. A. Ruden, A. Sanchez, T. Saue, S. P. A. Sauer, B. Schimmelpfenning, K. O. Sylvester-Hvid, P. R. Taylor, and O. Vahtras

- [11] W. Klemperer, W.G. Norris, A. Buchler, A.G. Emslie, J. Chem. Phys. 33 (1960) 1534. G.L. Vidale, J. Phys. Chem. 64 (1960) 314. K.P. Vasilevskii, V.I. Baikov, V.I., Opt. Spectrosc. Engl. Transl. 11 (1961) 21, in original 41.
- [12] D.-W. Chen, K.N. Rao, R.S. McDowell, J. Mol. Spectrosc. 61 (1976) 71.
- [13] D.C. Cartwright, T.H. Dunning Jr., J. Phys. B 7 (1974) 1776.
- [14] H.G.M. Edwards, E.A.M. Good, D.A. Long, J. Chem. Soc. Faraday Trans. 2 72 (1976) 984-987.
- [15] Ö. Legeza, J. Röder, B.A. Hess, Phys. Rev. B 67 (2002) 125114.
- [16] Ö. Legeza, J. Röder, B.A. Hess, Mol. Phys 101 (2003) 2019.
- [17] G. Moritz, B.A. Hess, M. Reiher, J. Chem. Phys. 122 (2005) 024107.
- [18] Ö. Legeza, J. Sólyom, Phys. Rev. B 70 (2004) 205118.
- [19] W.H. Press, S.A. Teukolsky, W.T. Vetterling, B.P. Flannery, Numerical recipes in C++, Cambridge, University Press, 2002.
- [20] S. Daul, I. Ciofini, C. Daul and S. R. White, Int. J. Quantum Chem. 79 (2000) 331.